The Influence of Synoptic-Scale Wind Patterns on Column-Integrated Nitrogen Dioxide, Ground-Level Ozone, and the Development of Sea-Breeze Circulations in the New York City Metropolitan Area

DILCHAND NAUTH,[a] CHRISTOPHER P. LOUGHNER,[b] AND MARIA TZORTZIOU[a]

[a] *Earth and Atmospheric Sciences Department, City University of New York, New York, New York*
[b] *NOAA/Air Resources Laboratory, College Park, Maryland*

(Manuscript received 7 September 2022, in final form 7 February 2023, accepted 14 February 2023)

ABSTRACT: The continually changing atmospheric conditions over densely populated coastal urban regions make it challenging to produce models that accurately capture the complex interactions of anthropogenic and environmental emissions, chemical reactions, and unique meteorological processes, such as sea- and land-breeze circulations. The purpose of this study is to determine and identify the influence of synoptic-scale wind patterns on the development of local-scale sea-breeze circulations and air quality over the New York City (NYC), New York, metropolitan area. This study utilizes column-integrated nitrogen dioxide observations made during the Long Island Sound Tropospheric Ozone Study (LISTOS) field campaign, ground-level ozone observations, the HRRR numerical weather prediction model, and trajectory model simulations using the NOAA HYSPLIT model. A cluster analysis within the HYSPLIT modeling system was performed to determine that there were six unique synoptic-scale transport pathways for NYC. Stagnant conditions or weak transport out of the northwest resulted in the worst air quality for NYC. Weak synoptic-scale forcings associated with these conditions allowed for local-scale sea-breeze circulations to develop, resulting in air pollution being able to recirculate and mix with freshly emitted pollutants.

SIGNIFICANCE STATEMENT: The purpose of this work is to understand how synoptic-scale wind patterns influence air quality and sea-breeze circulations in the New York City, New York, metropolitan area. This work shows that clean air can be imported into the region from rural New England and over the Atlantic Ocean, whereas polluted air can be transported into the region from the northwest and southwest. This work also shows the importance of the strength in synoptic-scale forcings in the development of sea-breeze circulations. Weak synoptic-scale winds allow for strong sea-breeze circulations to develop over all coastlines in the New York City region, resulting in air pollutants recirculating and mixing with freshly emitted air pollution and contributing to poor air quality.

KEYWORDS: Air quality; Coastal meteorology; Ozone; Regional models; Semi-Lagrangian models

1. Introduction

Coastal urban regions around the world are characterized by highly dynamic atmospheric composition influenced by meteorological processes unique to land–ocean interfaces, including sea/land-breeze circulations (Loughner et al. 2014; Geddes et al. 2021). Differences in heat capacities between large bodies of water and the surrounding landmass allow for differences in atmospheric temperature and pressure to occur, creating sea, bay, or lake breezes during the daytime. Sea breezes are most frequent in the summer months and can have a major impact on the spatial and temporal distribution of atmospheric pollution, aerosol particles, and trace gases such as nitrogen dioxide (NO_2) and ozone (O_3) in coastal urban areas (Loughner et al. 2016).

Strong changes in atmospheric composition, as a result of sea-breeze events, have been reported over dynamic coastal environments in Portugal, California, Asia, and parts of the United States as shown in field campaigns and extensive observational analyses (Evtyugina et al. 2006; Boucouvala and Bornstein 2003; Banta et al. 2005; Darby 2005; Loughner et al. 2014, 2016). These cases show that sea-breeze circulations contribute to poor air quality. Several studies show that stagnant conditions during days when a sea breeze is present result in a buildup of local surface constituents that persist throughout the day (Geddes et al. 2021; Loughner et al. 2011). Atmospheric chemistry, transportation of local emissions, smog, and thunderstorms are all influenced by sea-breeze circulations (Banta et al. 2005; Loughner et al. 2014; Wang and Kwok 2003; Chen et al. 2014), thus the need to thoroughly comprehend its importance over complex, dynamic coastal environments is ever demanded.

A prime example of an ever-changing coastal region influenced by both nearshore natural processes and anthropogenic activities is the New York City (NYC), New York, metropolitan area. Located along the northeastern coast of the United States, this large and densely populated metropolis encompasses the southern portion of New York State including NYC, Long Island, and parts of the Hudson Valley, and several large cities in both New Jersey and Connecticut including

Denotes content that is immediately available upon publication as open access.

Corresponding author: Christopher P. Loughner, christopher.loughner@noaa.gov

DOI: 10.1175/JAMC-D-22-0145.1

Newark and Jersey City, New Jersey, and New Haven and Bridgeport, Connecticut. This area is home to over 20 million residents and is surrounded by large bodies of water including the New York–New Jersey Bight, Atlantic Ocean, Hudson River, and Long Island Sound (LIS). Surface ozone pollution and emissions of ozone precursors—nitrogen oxides (NO_x) and volatile organic compounds (VOCs)—in the NYC metropolitan area and locations downwind are of particular interest because persistently high O_3 concentrations pose a threat to ecosystem and human health across the region. Despite significant improvements in air quality across the United States, the NYC metropolitan region experiences among the highest national NO_2 levels (Tzortziou et al. 2022) and continues to persistently violate national ambient air quality standards for ground-level ozone (Karambelas 2020).

Previous studies have found that wind speed, wind direction, and sea-breeze development can impact surface air quality in the NYC metropolitan area. Masiol et al. (2017) found that there was a higher probability of elevated surface concentrations of primary air pollutants under calm winds (<5 m s^{-1}). Higher wind speeds were correlated with minimal concentrations of local emitted species. Masiol et al. (2017) also performed a series of Hybrid Single-Particle Lagrangian Integrated Trajectory (HYSPLIT) trajectory simulations to find that the highest probability of distant air pollution emission sources impacting NYC originated within the eastern United States, particularly the upper Ohio River Valley region. Tzortziou et al. (2022) found a correlation between high total column NO_2 ($TCNO_2$) observed over NYC and low wind speeds. In addition, Tzortziou et al. (2022) found a correlation between the frequency of high NO_2 pollution events and wind direction with high observed $TCNO_2$ typically when winds were from the southeast, west, or southwest transporting pollutants from Queens and Brooklyn, New York (southeast); lower Manhattan, New York; and northern New Jersey (southwest–west). Zhang et al. (2022) examined ozone pollution over Long Island and found that high ozone days over the north shore of Long Island were characterized by calm conditions to begin the day, a sea-breeze front originating from south Long Island diverting a high ozone plume to the north shore, and stagnation of the sea-breeze front over Long Island north shore for several hours. High ozone for the south shore of Long Island were characterized by westerly or southwesterly flow transporting ozone and ozone precursors over the water and a sea breeze developing transporting high ozone from over the water inland Zhang et al. (2022).

The Long Island Sound Tropospheric Ozone Study (LISTOS) was launched in 2018, driven by the need to measure and understand the main processes influencing air quality, ozone formation, and pollution transport in the NYC region and areas downwind (NESCAUM 2021). To better comprehend the evolution, variability, and patterns of O_3 formation and transport in this region, the LISTOS campaign integrated measurements from different platforms, including satellite sensors, aircraft, ground-based sites, moving vehicles, and research vessels, to study the physical and chemical processes along this land–ocean interface that contribute to high O_3 concentrations (NESCAUM 2021). Led by the Northeast States for Coordinated Air Use Management (NESCAUM), LISTOS was a collaborative effort involving several state and federal agencies along with academic research institutions, including the City College of New York; Stony Brook University; the University of Albany; the University of Maryland, College Park; Yale University; the National Aeronautics and Space Administration (NASA); the National Oceanic and Atmospheric Administration (NOAA); the U.S. Environmental Protection Agency (EPA); the Connecticut Department of Energy and Environmental Protection (CDEEP); the Maine Department of Environmental Protection (MDEP); the New Jersey Department of Environmental Protection (NJDEP); and the New York State Department of Environmental Conservation (NYSDEC).

While previous studies have examined the impact of local-scale meteorology on air quality in NYC (Masiol et al. 2017; Tzortziou et al. 2022; Zhang et al. 2022) and the potential for long range transport of air pollutants into the NYC area, we examined the influence of synoptic-scale patterns on air quality as well as the influence of synoptic-scale meteorology on the development of sea-breeze circulations, which can contribute to poor air quality. Here, we integrated ground-based measurements during LISTOS with atmospheric model simulations to examine how meteorology, and specifically wind patterns and the development of sea-breeze events, influence the variability of total column NO_2 ($TCNO_2$) and surface ozone concentrations in this highly dynamic coastal environment. Multiple backward trajectory model simulations were run using the HYSPLIT model driven by the High-Resolution Rapid Refresh (HRRR) model, to capture the origin and transport of high ozone and NO_2 plumes over the NYC region. Combining surface and column-integrated NO_2 and surface O_3 observations with HYSPLIT model trajectory simulations allowed to categorize transport processes within the NYC metropolitan area during the peak measurement time period of the LISTOS field campaign (July–August 2018) and characterize favorable meteorological regimes for the development of sea-breeze circulations and high air pollution buildup.

2. Methods

a. *Study site (NYC metropolitan area)*

The NYC metropolitan area is one of the most densely populated urban environments in the United States, comprising multiple commercial, industrial, and residential zones intertwined with numerous jurisdictions and municipalities, including boroughs, cities, and suburbs. To characterize the variability of $TCNO_2$ and ground-level O_3, we used measurements from a network of ground-based instruments at key locations that allowed us to capture strong gradients in air quality across the study region. These included the Pandora spectrometer instruments (PSIs), sponsored by NASA and the European Space Agency (ESA), and surface air quality monitors from the EPA's Air Quality System (AQS), which are described below. The locations of these instruments (Fig. 1) collectively represent the study area and demonstrate the importance of localized emissions, including those from major NO_2 polluters, natural and anthropogenic sources, and transport of polluted air parcels influenced by wind.

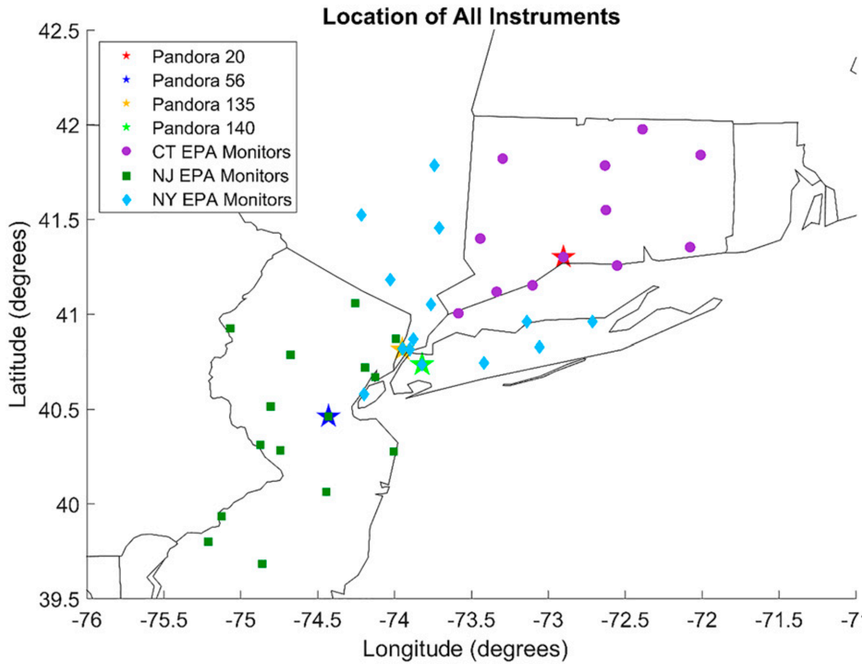

FIG. 1. Locations of all of the PSIs and EPA AQS monitors in the NYC metropolitan area used in this study.

The NOAA HYSPLIT model (Stein et al. 2015) was used to pinpoint the origins of air parcel trajectories and illustrate transport into the NYC metropolitan area and across key NO_2 emitted sources. To examine the development of sea-breeze circulations and the movement of the sea-breeze front across this urban coastal environment, we analyzed surface wind velocities from the HRRR meteorological model. The HYSPLIT and HRRR models are described below.

b. Measurements of TCNO$_2$ and surface O$_3$

1) PSI RETRIEVALS

Sponsored by NASA and ESA, the Pandonia Global Network (PGN) provides real-time, standardized, calibrated, and verified air quality data, and associated uncertainty values, from a network of ground-based UV–visible spectrometers, the PSIs (Herman et al. 2019). The PGN global network serves as a validation resource for UV–visible satellite sensors (e.g., Herman et al. 2009; Baek et al. 2020; Verhoelst et al. 2021), and Pandora sensors have been used widely for characterizing upper air pollutants under the U.S. EPA Photochemical Assessment Monitoring Stations (PAMS) program (Szykman et al. 2019).

The technical specifications of the Pandora instrument are described in Tzortziou et al. (2022). Briefly, the Pandora instrument is driven by a highly accurate sun tracker that points an optical head at the sun and transmits the received light to an Avantes low stray light charge-coupled device (CCD) spectrometer (spectral range: 280–525 nm; spectral resolution: 0.6 nm with 4 times oversampling) through a fiber optic cable (Herman et al. 2019; Tzortziou et al. 2014, 2022). Trace gas abundances along the light path are determined using differential optical absorption spectroscopy. The system can operate in both direct-sun and sky-scan mode for retrievals of O_3, NO_2, SO_2, and CH_2O total columns and provides information on the vertical profiles of these trace gases (Tzortziou et al. 2012; Herman et al. 2019; Spinei et al. 2018). These data can be used to study the composition of the atmosphere and behavior of trace gases across a range of temporal scales, from diurnal to seasonal cycles and interannual variability. This paper discusses Pandora retrievals of total column amounts of NO_2 ($TCNO_2$) using direct-sun observations. The estimated $TCNO_2$ error in Pandora retrievals is approximately 0.05 Dobson units (DU; Herman et al. 2019).

In this study, we used data from four ground-based Pandora instruments located in Manhattan (PSI 135); New Haven (PSI 20); New Brunswick, New Jersey (PSI 56); and Queens (PSI 140), to examine NO_2 dynamics across the tri-state New Jersey–New York–Connecticut region. PSI 135 is located at N 40°48′55.08″ W 73°57′1.8″, 34 m above ground level on the City University of New York (CUNY) Advanced Science Research Center (ASRC) building roof on the City College of New York (CCNY) campus in West Harlem, Manhattan. PSI 20 is located at 41°18′5.04″N 72°54′10.44″W, 4 m above ground level in Criscuolo Park, New Haven. PSI 56 is located at 40°27′43.92″N 74°25′45.84″W, 19 m above ground level on the Rutgers University campus, in New Brunswick. PSI 140 is located at 40°44′9.96″N 73°49′17.4″W, 25 m above ground level on the Queens College campus in Queens. Pandora data were filtered here for solar zenith angle less than 70°, normalized root-mean-square error of weighted spectral fitting residuals less than 0.05, and uncertainty in NO_2 retrievals less than 0.1 DU.

2) EPA AQS

The Air Quality System contains ambient air pollution data collected by the EPA, state, local, and tribal air pollution control agencies, to assess the levels and distribution of six criteria pollutants–$PM_{2.5}$, PM_{10}, O_3, CO, SO_2, NO_2, and Pb (Lutz 2002). The data submitted to the AQS are required to meet certain regulations, increasing its reliability and accuracy, and is used for assessing air quality, developing State Implementation Plans, modeling for permit review analysis, and preparing reports as mandated by the Clean Air Act (EPA 2020). It can be further used for studying the composition of the atmosphere and behavior of these criteria pollutants. Preprocessed data from the EPA AQS were acquired from the EPA's Outdoor Air Quality Data tool (EPA 2018). Forty-three EPA AQS monitors located throughout the NYC metropolitan area, including the Long Island Sound, the five boroughs of NYC, northern New Jersey, and the state of Connecticut, were used to create products that assisted in a visual analysis of how surface O_3 concentrations and patterns varied for different meteorological transport regimes.

3) NOAA HYSPLIT MODEL

NOAA's HYSPLIT model is a complete system capable of computing simple air parcel trajectories, complex transport, chemical transformation, complex dispersion, and deposition simulations within Earth's atmosphere (Stein et al. 2015). HYSPLIT can use a hybrid calculation method between the Lagrangian and Eulerian approaches, applying both a shifting frame of reference relative to the location of the air parcels with respect to those parcels' initial position and a fixed 3D grid as a frame of reference, respectively. Advection and dispersion algorithms, as well as modules for chemical transformations and deposition, assist in developing simulations that allow for the better comprehension of atmospheric transport and dispersion of pollutants, hazardous materials, and deposition of materials across Earth's surface (Stein et al. 2015). The HYSPLIT model is pertinent in a wide range of applications, including forecasting the transport of wildfire smoke, volcanic ash, windblown dust, and nuclear material and other hazardous pollutants emitted from stationary and mobile sources (Stein et al. 2015).

HYSPLIT backward-in-time trajectories were initialized at 1800 UTC for each day between 1 July and 31 August 2018. The trajectories were initialized at 500 m AGL and run 12 h backward in time. A standard trajectory cluster analysis (Stein et al. 2015) with a 12-h cluster and 1-h time interval were inputted to produce a clustering file that categorized each day into unique clusters. A cluster is a group of select trajectories categorized by the HYSPLIT model based on similarities relative to each other. The total spatial variance (TSV) or the sum of the cluster spatial variance (CSV) over all the clusters allowed for a unique number of cluster selections, further producing the cluster means and individual trajectories within each cluster. The CSV is the sum of the spatial variances of the trajectories within a particular cluster. The clusters were analyzed to determine which clusters were more susceptible to poor air quality and sea-breeze circulations during the LISTOS field campaign. This work is the first cluster analysis for the NYC metropolitan area that relates synoptic-scale wind patterns to air quality and local-scale sea-breeze circulations.

4) HRRR MODEL

The HRRR atmospheric model was used in this study to drive HYSPLIT model simulations. The HRRR model is a high-resolution atmospheric model, developed by the NOAA Earth System Research Laboratory (ESRL) that allows for accurate short-term forecasts. The algorithm of HRRR contains an assimilation system and numerical forecast model and is run continually with a horizontal resolution of 3 km and has 50 vertical levels (Alexander 2021). Previous research has shown that meteorological models with a horizontal resolution coarser than about 4.5 km may not be capable of capturing sea-breeze circulations (Loughner et al. 2011). The HRRR model has a high enough spatial resolution to capture these localized circulation patterns. With the influence of onshore and offshore surface winds over the NYC metropolitan area, HRRR provides detailed products allowing for the further analysis of wind patterns that affect the movement of polluted air parcels over the area.

3. Results and discussion

Daily HYSPLIT backward trajectory simulations initialized at 1800 UTC from PSI 135 between 1 July and 31 August 2018 were clustered using the TSV. The TSV values, which arise from calculating the sum of all the cluster spatial variances, change minimally as the number of clusters decrease from 30 to 6, suggesting there is little benefit in utilizing more than 6 clusters (Fig. 2). There is a sharp increase in TSV from six clusters to five, indicating that the clusters being grouped are no longer similar. Therefore, six clusters were chosen for this study. The cluster means and individual trajectories for each cluster are shown in Figs. 3 and 4, respectively.

The near-northwest cluster, southwest cluster, and far-northwest cluster in Fig. 4 account for 57% of the trajectories that originated from the west, northwest, and southwest relative to the location of PSI 135, respectively. The origins and direction of these clusters reveal that though these mean trajectories were influenced by westerly winds, all trajectories traveled over or near major NO_2 polluters located near and west of the location of PSI 135. The local cluster (Fig. 4), which accounts for 26% of the trajectories, shows that source regions for these days originated extremely close to the location of PSI 135. The northeast cluster (Fig. 4), accounts for 11% of the trajectories and originated from the northeast relative to the location of PSI 135, while the south cluster (Fig. 4), accounts for 6% of the trajectories and originated from the south of PSI 135 over the Atlantic Ocean. The local cluster reveals that 16 backward trajectories originated from the local area around the NYC metropolitan area, including over the LIS and the five boroughs of New York. A statistical analysis, shown in Figs. 5a and 5b shows the highest amount of NO_2 corresponding to the local cluster. Stagnation or weak surface

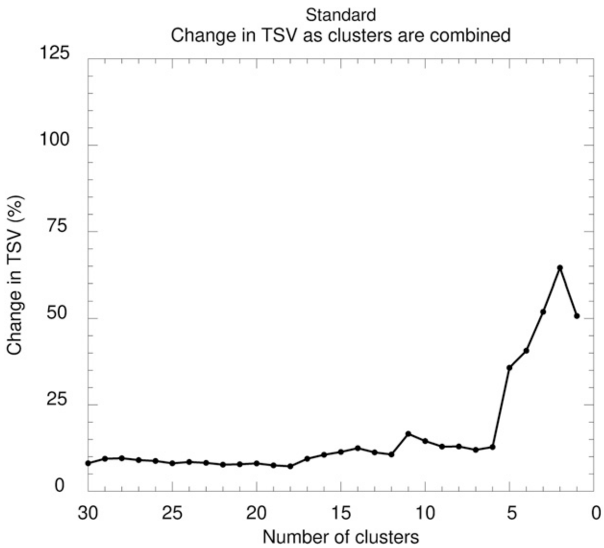

FIG. 2. Standard TSV from the HYSPLIT cluster analysis, showing the change in TSV percentage as the number of clusters are combined.

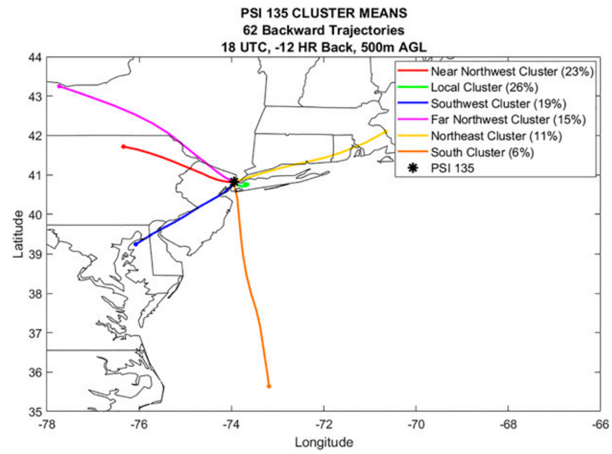

FIG. 3. Individual cluster means with a start time of 1800 UTC at 500 m AGL, going backward 12 h from the start time. The percentages represent the number of trajectories, of the 62 total trajectories, within each cluster. The black asterisk represents the location of the Pandora instrument in Manhattan (PSI 135).

winds allowed for pollutants to accumulate in the NYC metropolitan area on days represented by the local cluster.

$TCNO_2$ observations for PSI 135 show that the local cluster, associated with low wind speed conditions, has the highest average (0.92 DU) and maximum (4.59 DU) values when compared with the other mean cluster trajectories (Figs. 5a,b). $TCNO_2$, which is calculated as the sum of stratospheric and tropospheric NO_2 column, can be attributed to anthropogenic activities, including the use of air conditioning units, vehicle traffic, and burning of fossil fuels in power plants. Because the air over the local cluster was stagnant and there were low wind speeds persisting over the NYC metropolitan area for these days, NO_2 emitted from these activities accumulated and remained over the area close to the location of PSI 135.

The southwest cluster had the second highest daily average and daily maximum $TCNO_2$ (0.67 and 1.74 DU, respectively, Figs. 5a,b). These results are in agreement with Tzortziou et al. (2022), who found that meteorological conditions on days when high $TCNO_2$ was measured in Manhattan—even shortly after the COVID-19 pandemic restrictions were imposed—were characterized by low-speed, southwesterly winds. The mean trajectory of this cluster follows the I-95 interstate highway corridor from Washington, D.C., to New York City passing over or close to Baltimore, Maryland; Philadelphia, Pennsylvania; and urban and industrialized portions of New Jersey.

The near-northwest cluster passes over industrialized and urban northern New Jersey and had the third highest daily average and daily maximum $TCNO_2$ (0.51 and 1.73 DU, respectively, Figs. 5a,b). The far-northwest, northeast, and south clusters had the lowest $TCNO_2$ values. Although the far-northwest cluster also passes over northern New Jersey, the higher wind speeds associated with these trajectories allow for the pollutants from northern New Jersey to disperse faster. In addition, these stronger synoptic-scale winds suppressed the formation of localized sea-breeze circulations and air pollution recirculation and accumulation associated with these localized coastal circulations. The trajectories associated with the northeast cluster originate from rural northern New England and the trajectories associated with the south cluster originate from over the ocean transporting low NO_2 marine air masses.

The daily maximum 8-h-average surface O_3 for the EPA AQS monitor on Manhattan, which is 1200 ft (<370 m) from PSI 135, shows that the near-northwest, local, southwest, and far-northwest clusters have higher amounts of average and maximum surface O_3 relative to the northeast and south clusters (Figs. 5c,d). Although the near-northwest, southwest, and far-northwest mean clusters are not stagnant, results reveal that the direction of travel is over areas where O_3 precursors are emitted, such as NO_x from urban and industrial sources and roadways. The southwest cluster, for example, travels near the I-95 interstate highway, which is an area of consistent traffic movement and volume throughout the day. Similarly, the near-northwest and far-northwest clusters travel near major roadways and over major power plants in northern New Jersey. The northeast and south clusters originate from rural areas or over the ocean with minimal ozone precursor emissions.

The highest average (Fig. 6) and maximum (Fig. 7) $TCNO_2$ values occur in the most densely populated locations in the NYC metropolitan area. The highest average and maximum $TCNO_2$ for the near-northwest, local, southwest, far-northwest, and northeast measured by the Pandora instruments were in Manhattan and Queens, respectively. The highest recorded average $TCNO_2$ (greater than 0.9 DU) was in the local cluster, where stagnation persisted. Maximum recorded $TCNO_2$ (greater than 1.3 DU) for PSIs 135 and 140 was also found in the local cluster. The lowest average and maximum $TCNO_2$ amounts were found at all PSI locations in the northeast and south clusters, trajectories that originate and travel over less polluted areas.

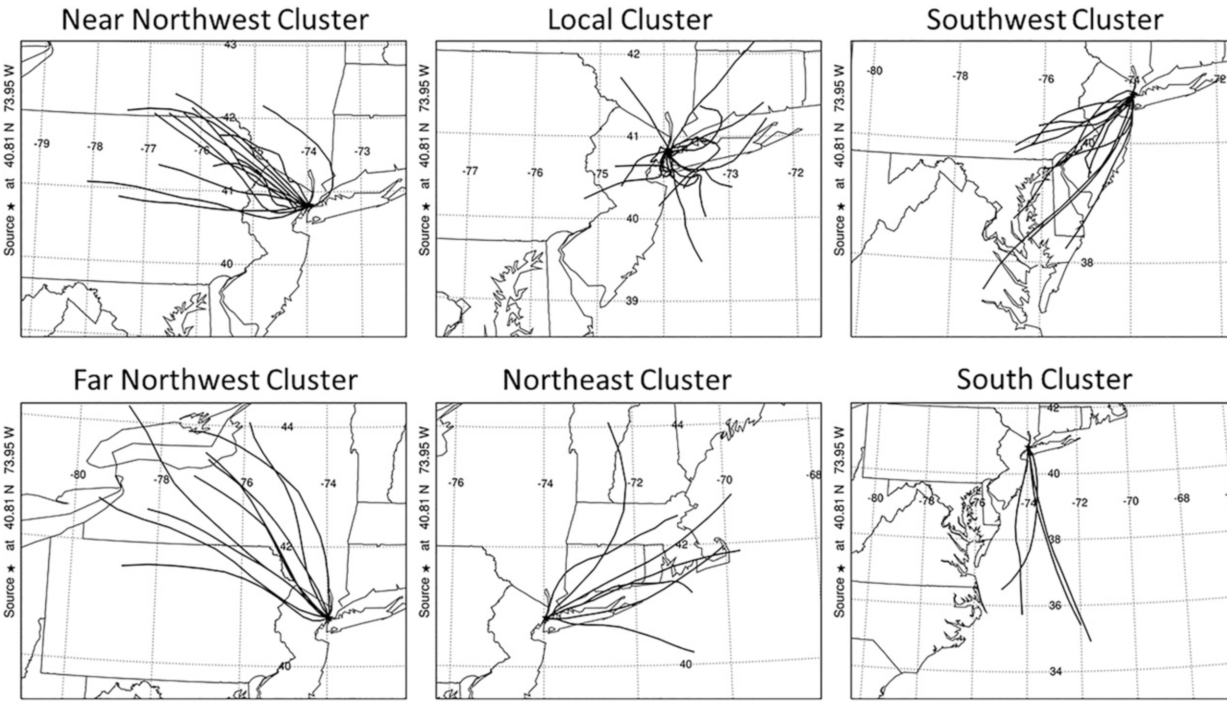

FIG. 4. Individual trajectories within each unique cluster.

With more instruments available for measuring surface O_3, a wider representation of spatial variability of surface ozone in the NYC metropolitan area is represented for each cluster in Figs. 8 and 9. Surface O_3 in the near-northwest and local clusters are classified as having the highest average and maximum amounts of surface O_3 followed by the southwest and far-northwest clusters. The northeast and south clusters have the least amount of surface O_3.

The stagnant winds in the local cluster are associated with weak synoptic-scale forcing. Localized forcing from the temperature gradient at the land water interface dominates when the synoptic-scale winds are weak. Therefore, sea-breeze circulations are common for the local cluster. Maps of HRRR simulated 10-m wind velocity were analyzed throughout the 2-month study period to identify days when sea breezes occurred within the NYC metropolitan area. Sea-breeze days were detected by identifying sea-breeze fronts by recognizing surface convergence from the HRRR near surface wind velocities. Strong sea breezes when the sea breeze penetrated far inland, as well as weak sea breezes, when the convergence zone was identified along the coastline, but did not penetrate far inland, were counted as sea-breeze days. Table 1 shows that 100% of local cluster days during our study period were sea-breeze days.

An example of midday wind patterns for a local cluster day is shown in Fig. 10 (upper-left panel) for 5 August 2018, depicting sea-breeze circulation along the entire New Jersey–New York–Connecticut coastline, including the northern and southern coastlines of Long Island. Afternoon sea breezes are also common along these coastlines for the near-northwest cluster, which features weak northwesterly synoptic-scale winds. Sea-breeze days occurred 93% of near-northwest cluster days within this 2-month study period (Table 1). An example of afternoon winds for a near-northwest cluster day is shown in Fig. 10 (upper-right panel). When regional synoptic-scale forcings are weak, local-scale forcings can dominate circulation patterns. For the local and near-northwest clusters, sea breezes dominate the afternoon circulation patterns. Sea-breeze circulations cause pollutants to stagnate as the wind changes direction and recirculate and mix with freshly emitted pollutants (Banta et al. 2005; Loughner et al. 2011, 2016). This results in some of the highest surface ozone concentrations to occur in the NYC area under the local and near-northwest clusters.

For the southwest cluster, the synoptic-scale winds are close to parallel with the New Jersey coastline. Of the 14 days under the southwest cluster regime, only one day consisted of sea-breeze circulations along the New Jersey, Long Island, and Connecticut coastline, similar to the sea-breeze circulations simulated under the local and near-northwest clusters. For all other days in the southwest cluster regime, either only a weak sea breeze or no sea breeze was simulated with the HRRR model along the New Jersey coastline (example shown in Fig. 10, lower-left panel). The localized forcings were not strong enough to overtake the moderate synoptic-scale winds for 11 of the 12 southwest cluster days in order to have the winds turn almost 180° to form a sea breeze along the northern coastline of Long Island. Sea breezes occurred 58% of the time for the southwest cluster (Table 1). The highest ozone concentrations were found

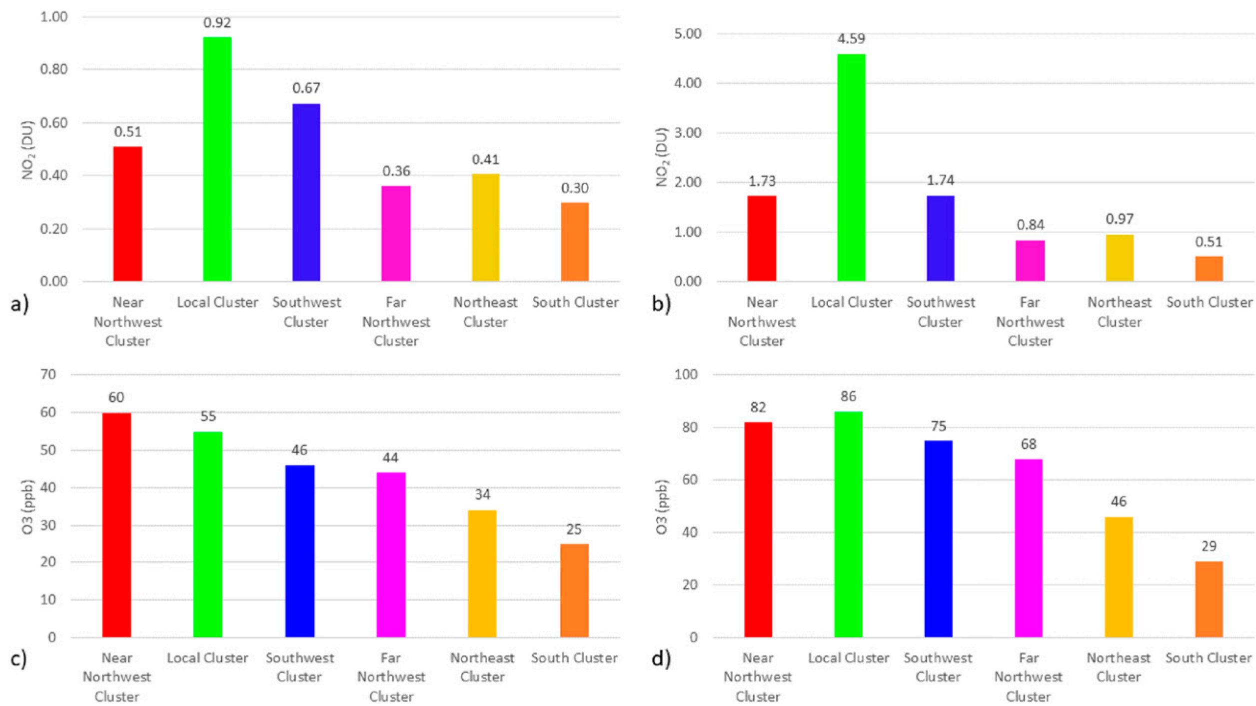

FIG. 5. Daily (a),(c) average and (b),(d) maximum of the (top) $TCNO_2$ (DU) at the location of PSI 135 and of the (bottom) maximum 8-h-average surface O_3 (ppb; this EPA ozone instrument is located roughly 1200 ft away from the location of PSI 135) associated with each cluster of trajectories shown in Fig. 4, which had a start time of 1800 UTC each day.

downwind of NYC in Connecticut for the southwest cluster (Figs. 8 and 9).

Trajectories for the far-northwest cluster pass over northern New Jersey, just like the near-northwest cluster trajectories. However, as discussed previously, the synoptic-scale winds were stronger in the far-northwest cluster preventing strong sea breezes from forming. Of the 9 days under the far-northwest cluster regime, the HRRR simulated 4 days with weak sea

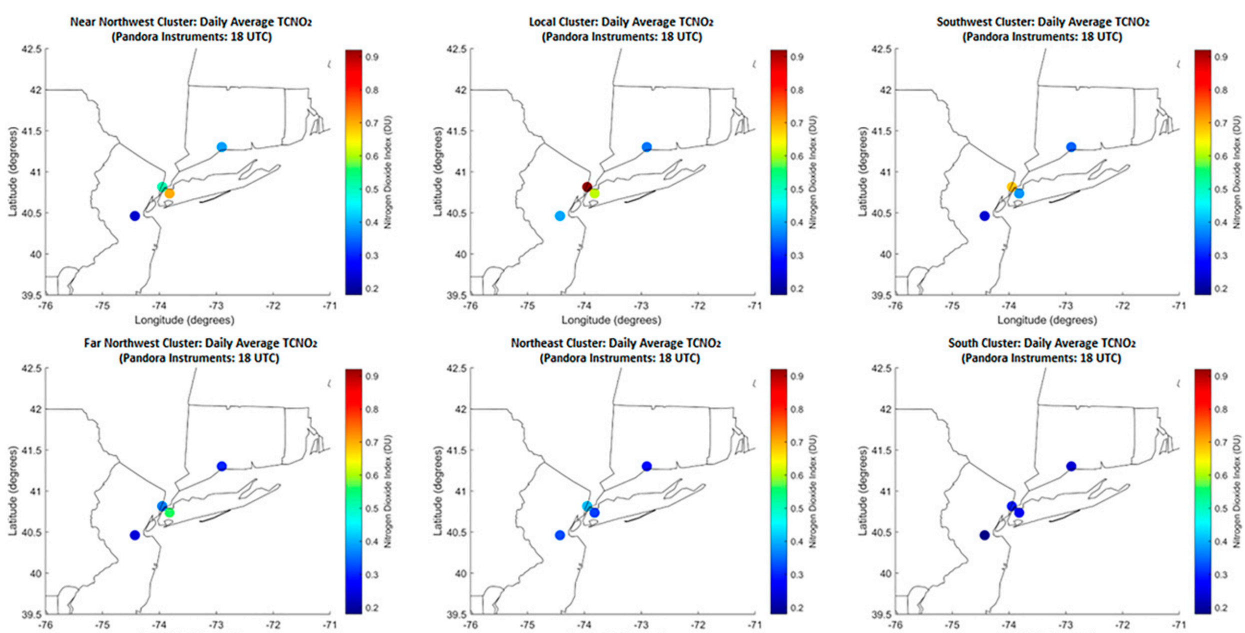

FIG. 6. Daily average $TCNO_2$ associated with each cluster of trajectories, which had a start time of 1800 UTC each day, for each ground-based PSI instrument in the LISTOS campaign across the NYC metropolitan area.

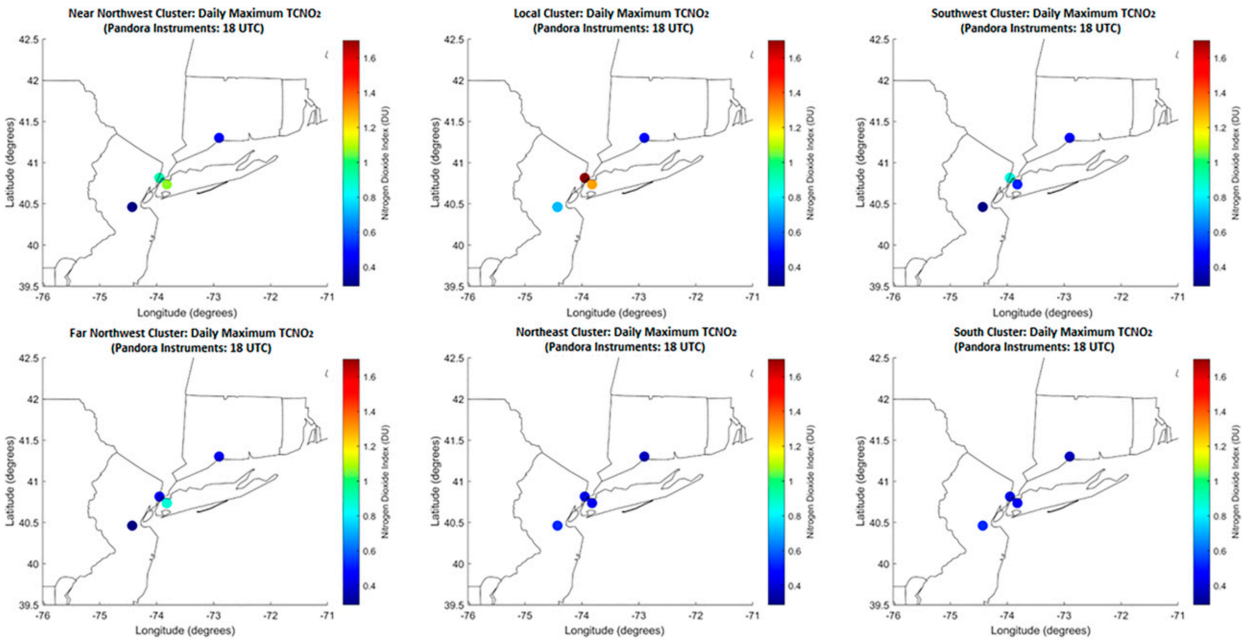

FIG. 7. As in Fig. 6, but for daily maximum $TCNO_2$ (i.e., the single biggest value for the 2-month period at each site).

breezes along the southern coastline of Long Island and the Connecticut coastline (an example is shown in Fig. 10, lower-right panel). No sea breezes were simulated for the other 5 days for the far-northwest cluster.

Weak sea breezes were simulated 3 of the 7 northeast cluster days, and no sea breezes were simulated during south cluster days (Table 1). Moderate-to-strong wind velocities were prevalent during northeast and south cluster days. Sea-breeze days were simulated 69% of the days during the 2-month study period.

4. Conclusions

Surface based observations of $TCNO_2$ and ground-level O_3, HYSPLIT trajectory simulations, and the HRRR model were used to identify synoptic-scale regimes that are susceptible to

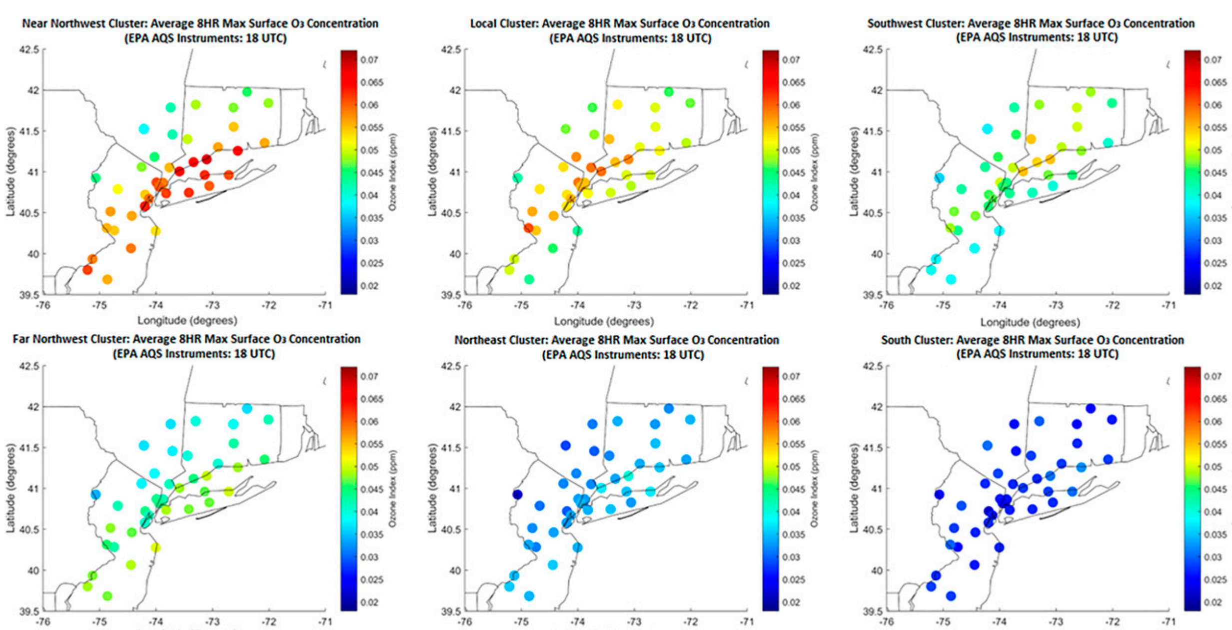

FIG. 8. Average of the daily maximum 8-h-average surface O_3 concentration associated with each cluster of trajectories, which had a start time of 1800 UTC each day, for several different EPA AQS monitors across the NYC metropolitan area.

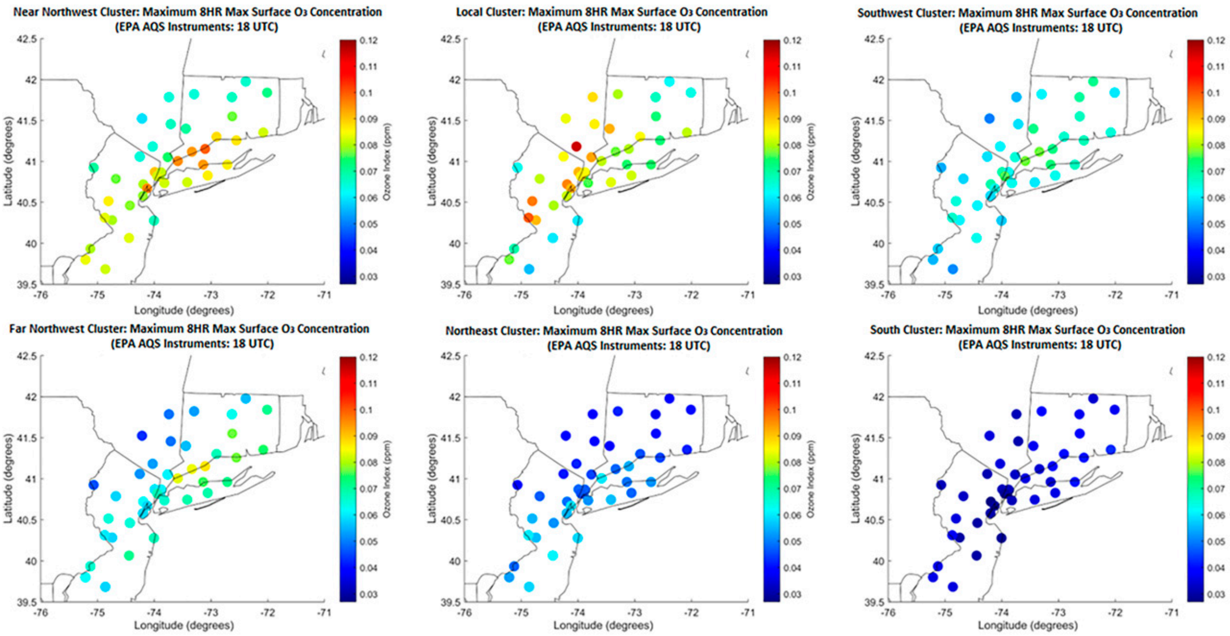

FIG. 9. As in Fig. 8, but for the 2-month maximum of the daily maximum 8-h-average surface O_3 concentration.

clean and dirty air days in the NYC metropolitan area. The HYSPLIT trajectory cluster analysis identified six main transport pathways into the NYC area. $TCNO_2$ and surface O_3 observations were analyzed for each of the six clusters to identify which transport pathways are more susceptible to poor air quality. Stagnant conditions (local cluster) and moderate southwest winds (southwest cluster) resulted in the highest $TCNO_2$ conditions over the NYC metropolitan area, in agreement with previous studies using Tropospheric Monitoring Instrument (TROPOMI) and Pandora measurements (Tzortziou et al. 2022). Stagnant conditions and weak transport from the northwest (near-northwest cluster) resulted in the highest surface ozone concentrations, followed by moderate synoptic-scale winds from the southwest (southwest cluster) and northwest (far-northwest cluster). Stagnant conditions allowed for local air pollution emissions to build up in the area. Winds from the northwest transport pollution from the heavily industrialized and urban areas northwest of NYC, and winds from the southwest transport pollutants along the I-95 corridor between the Washington, D.C.–Baltimore metropolitan area and NYC into the area of interest. Surface wind patterns were analyzed for each day within all clusters to identify which clusters are more likely to simulate sea-breeze circulations. Strong sea-breeze circulations developed on each day of the local cluster, which consisted of stagnant winds, and the near-northwest cluster, which is characterized by weak synoptic-scale winds passing over northern New Jersey. Sea-breeze circulations in a polluted environment cause pollutants to recirculate and converge with freshly emitted air pollutants along the sea-breeze convergence zone resulting in poor air quality. The longer transport paths represented by the far-northwest and southwest clusters indicate stronger synoptic-scale winds. These stronger regional-scale winds prevented strong local-scale sea-breeze circulations from developing. Either no sea breeze or a weak sea-breeze circulation along a coastline close to parallel with the synoptic-scale winds were simulated for cases under the far-northwest and southwest clusters. Clean air was prevalent under the northeast and south clusters, which transported air from over rural New England and the Atlantic Ocean, respectively.

This unique analysis combining high-resolution meteorological model output, HYSPLIT trajectory cluster analysis,

TABLE 1. Total number of days, number of days on which sea breezes were identified within the NYC metropolitan area, and the percentage of sea-breeze days within the 2-month study period for each cluster and all clusters combined. Sea-breeze days were identified by analyzing 10-m wind velocities from HRRR model output and identifying sea-breeze convergence zones along and near coastlines. Sea-breeze days include weak sea breezes that were present along a coastline and strong sea-breeze days when the convergence zone penetrated inland.

	Near-northwest cluster	Local cluster	Southwest cluster	Far-northwest cluster	Northeast cluster	South cluster	All clusters
No. of days	14	16	12	9	7	4	62
No. of sea-breeze days	13	16	7	4	3	0	43
Percentage of sea-breeze days	93%	100%	58%	44%	43%	0%	69%

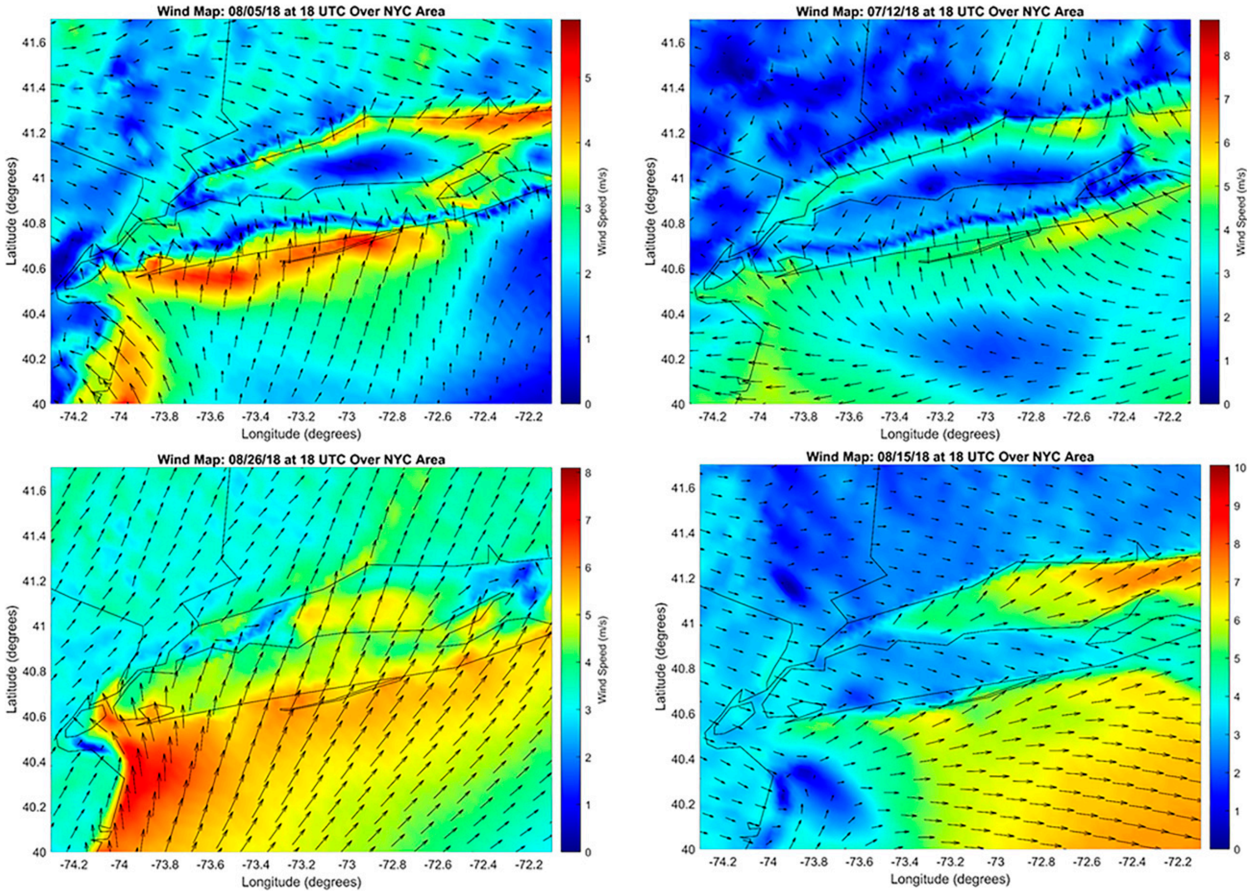

FIG. 10. HRRR model wind product at 1800 UTC over the NYC metropolitan area. Sea-breeze events typically develop in this region under (top left) near-northwest wind conditions and (top right) stagnant winds. (bottom left) The southwest cluster in our analysis was typically associated with high wind speeds over the LIS and location of the PSI and EPA AQS instruments, whereas (bottom right) moderate-to-low speeds are observed over the LIS and location of the PSI and EPA AQS instruments in most cases of the far-northwest cluster.

and observations from the LISTOS field campaign allows for the identification of transport pathways that impact the severity of air quality in the NYC metropolitan area. This work shows the importance of the strength in synoptic-scale forcing in the development, or lack of development, of local-scale sea-breeze circulations that influence air quality in the region. Strong synoptic-scale winds prevent local-scale sea-breeze circulations from developing; moderate synoptic-scale winds allow for weak sea-breeze circulations along a coastline close to parallel to the regional-scale wind flow; and weak synoptic-scale winds allow for strong sea-breeze circulations to develop over all coastlines in the area causing air pollutants to recirculate and mix with freshly emitted air pollution.

Acknowledgments. We thank Nader Abuhassan, Alexander Cede, Thomas Hanisco, Moritz Mueller, and the NASA Pandora Project and ESA Pandonia Project staff for assistance in the field and for establishing and maintaining the Pandora sites used in this investigation. This research was supported by NASA Applied Science Program, Grant NNX16AD60G, and NASA Interdisciplinary Science (IDS) Program, Grant 80NSSC17K0258. During the time that this paper was written, author Nauth was supported by the NOAA–Cooperative Science Center for Earth System Sciences and Remote Sensing Technologies (CESSRST) under the Cooperative Agreement Grant NA16SEC4810008. Nauth thanks the NOAA Educational Partnership Program with Minority Serving Institutions for fellowship support. The statements contained within this paper are not the opinions of the funding agency or the U.S. government but reflect the authors' opinions.

Data availability statement. HYSPLIT, version 5.0.0, (https://www.ready.noaa.gov/HYSPLIT.php) and HYSPLIT formatted HRRR files (https://www.ready.noaa.gov/archives.php) are available online. All Pandora data used in this study including column-integrated nitrogen dioxide from PSIs can be downloaded freely from the Pandonia Global Network (https://www.pandonia-global-network.org) and by contacting Maria Tzortziou (mtzortziou@ccny.cuny.edu). All ozone data including daily maximum 8-h-average ozone observations from EPA AQS monitors can be downloaded freely from the U.S. Environmental

Protection Agency Outdoor Air Quality website (https://www.epa.gov/outdoor-air-quality-data/download-daily-data).

REFERENCES

Alexander, C., 2021: The High-Resolution Rapid Refresh Model (HRRR). NOAA/Global Systems Laboratory, accessed 15 July 2022, https://rapidrefresh.noaa.gov/hrrr/.

Baek, K., J.-H. Kim, and J. Kim, 2020: The cross-validation of satellite OMI and OMPS total ozone with Pandora measurement. *Korean J. Remote Sens.*, **36**, 461–474, https://doi.org/10.7780/kjrs.2020.36.3.6.

Banta, R. M., and Coauthors, 2005: A bad air day in Houston. *Bull. Amer. Meteor. Soc.*, **86**, 657–670, https://doi.org/10.1175/BAMS-86-5-657.

Boucouvala, D., and R. Bornstein, 2003: Analysis and transport patterns during an SCOS97-NARSTO episode. *Atmos. Environ.*, **37**, 73–94, https://doi.org/10.1016/S1352-2310(03)00383-2.

Chen, T.-C., M.-C. Yen, J.-D. Tsay, C.-C. Liao, and E. S. Takle, 2014: Impact of afternoon thunderstorms on the land–sea breeze in the Taipei Basin during summer: An experiment. *J. Appl. Meteor. Climatol.*, **53**, 1714–1738, https://doi.org/10.1175/JAMC-D-13-098.1.

Darby, L. S., 2005: Cluster analysis of surface winds in Houston, Texas, and the impact of wind patterns on ozone. *J. Appl. Meteor.*, **44**, 1788–1806, https://doi.org/10.1175/JAM2320.1.

EPA, 2018: Outdoor air quality data. U.S. Environmental Protection Agency, accessed 15 July 2022, https://www.epa.gov/outdoor-air-quality-data/download-daily-data.

——, 2020: Air Quality System (AQS). U.S. Environmental Protection Agency, accessed 15 July 2022, https://www.epa.gov/aqs.

Evtyugina, M. G., T. Nunes, C. Pio, and C. S. Costa, 2006: Photochemical pollution under sea breeze conditions, during summer, at the Portuguese west coast. *Atmos. Environ.*, **40**, 6277–6293, https://doi.org/10.1016/j.atmosenv.2006.05.046.

Geddes, A. J., B. Wang, and D. Li, 2021: Ozone and nitrogen dioxide pollution in a coastal urban environment: The role of sea breezes, and implications of their representation for remote sensing of local air quality. *J. Geophys. Res. Atmos.*, **126**, e2021JD035314, https://doi.org/10.1029/2021JD035314.

Herman, J., A. Cede, E. Spinei, G. Mount, M. Tzortziou, and N. Abuhassan, 2009: NO_2 column amounts from ground-based Pandora and MFDOAS spectrometers using the direct-sun DOAS technique: Intercomparisons and application to OMI validation. *J. Geophys. Res.*, **114**, D13307, https://doi.org/10.1029/2009JD011848.

——, N. Abuhassan, J. Kim, J. Kim, M. Dubey, M. Raponi, and M. Tzortziou, 2019: Underestimation of column NO_2 amounts from the OMI satellite compared to diurnally varying ground-based retrievals from multiple PANDORA spectrometer instruments. *Atmos. Meas. Tech.*, **12**, 5593–5612, https://doi.org/10.5194/amt-12-5593-2019.

Karambelas, A., 2020: LISTOS: Toward a better understanding of New York City's ozone pollution problem. *EM*, **October 2020**, 10–16, https://www.awma.org/content.asp?admin=Y&contentid=657.

Loughner, C. P., D. J. Allen, K. E. Pickering, D.-L. Zhang, Y.-X. Shou, and R. R. Dickerson, 2011: Impact of fair-weather cumulus clouds and the Chesapeake Bay breeze on pollutant transport and transformation. *Atmos. Environ.*, **45**, 4060–4072, https://doi.org/10.1016/j.atmosenv.2011.04.003.

——, and Coauthors, 2014: Impact of bay-breeze circulations on surface air quality and boundary layer export. *J. Appl. Meteor. Climatol.*, **53**, 1697–1713, https://doi.org/10.1175/JAMC-D-13-0323.1.

——, M. Tzortziou, S. Shroder, and K. E. Pickering, 2016: Enhanced dry deposition of nitrogen pollution near coastlines: A case study covering the Chesapeake Bay estuary and Atlantic Ocean coastline. *J. Geophys. Res. Atmos.*, **121**, 14 221–14 238, https://doi.org/10.1002/2016JD025571.

Lutz, D., 2002: AQS basics: What data are in AQS? EPA Office of Air and Radiation, accessed 15 July 2022, https://www3.epa.gov/ttnairs1/airsaqsORIG/manuals/AQS%20Basics.pdf.

Masiol, M., P. K. Hopke, H. D. Felton, B. P. Frank, O. V. Rattigan, M. J. Wurth, and G. H. LaDuke, 2017: Analysis of major air pollutants and submicron particles in New York City and Long Island. *Atmos. Environ.*, **148**, 203–214, https://doi.org/10.1016/j.atmosenv.2016.10.043.

NESCAUM, 2021: Long Island Sound Tropospheric Ozone Study (LISTOS). Northeast States for Coordinated Air Use Management, accessed 15 July 2022, https://www.nescaum.org/documents/listos/faq.

Spinei, E., and Coauthors, 2018: The first evaluation of formaldehyde column observations by improved Pandora spectrometers during the KORUS-AQ field study. *Atmos. Meas. Tech.*, **11**, 4943–4961, https://doi.org/10.5194/amt-11-4943-2018.

Stein, F. A., R. R. Draxler, G. D. Rolph, B. J. B. Stunder, D. M. Cohen, and F. Ngan, 2015: NOAA'S HYSPLIT atmospheric transport and dispersion modeling system. *Bull. Amer. Meteor. Soc.*, **96**, 2059–2077, https://doi.org/10.1175/BAMS-D-14-00110.1.

Szykman, J., and Coauthors, 2019: Pandora: Connecting in-situ and satellite monitoring in support of the Canada–U.S. Air Quality Agreement. *EM*, **June 2019**, 29–35, https://www.awma.org/emjune19.

Tzortziou, M., J. R. Herman, A. Cede, and N. Abuhassan, 2012: High precision, absolute total column ozone measurements from the Pandora spectrometer system: Comparisons with data from a Brewer double monochromator and Aura OMI. *J. Geophys. Res.*, **117**, D16303, https://doi.org/10.1029/2012JD017814.

——, ——, Z. Ahmad, C. P. Loughner, N. Abuhassan, and A. Cede, 2014: Atmospheric NO_2 dynamics and impact on ocean color retrievals in urban nearshore regions. *J. Geophys. Res. Oceans*, **119**, 3834–3854, https://doi.org/10.1002/2014JC009803.

——, C. F. Kwong, D. Goldberg, L. Schiferl, R. Commane, N. Abuhassan, J. J. Szykman, and L. C. Valin, 2022: Declines and peaks in NO_2 pollution during the multiple waves of the COVID-19 pandemic in the New York metropolitan area. *Atmos. Chem. Phys.*, **22**, 2399–2417, https://doi.org/10.5194/acp-22-2399-2022.

Verhoelst, T., and Coauthors, 2021: Ground-based validation of the Copernicus Sentinel-5P TROPOMI NO_2 measurements with the NDACC ZSL-DOAS, MAX-DOAS and Pandonia global networks. *Atmos. Meas. Tech.*, **14**, 481–510, https://doi.org/10.5194/amt-14-481-2021.

Wang, T., and J. Y. H. Kwok, 2003: Measurement and analysis of a multiday photochemical smog episode in the Pearl River delta of China. *J. Appl. Meteor.*, **42**, 404–416, https://doi.org/10.1175/1520-0450(2003)042<0404:MAAOAM>2.0.CO;2.

Zhang, J., and Coauthors, 2022: Unraveling the interaction of urban emission plumes and marine breezes involved in the formation of summertime coastal high ozone on Long Island. *Environ. Sci. Atmos.*, **2**, 1438–1449, https://doi.org/10.1039/D2EA00061J.